



HAL
open science

Impact of the sizing reactivity of glass fibers on composites hydrothermal aging

Sigrid Assengone Ootogo Be, Lénaïk Belec, Armand Fahs, Isabelle Martin, Guy
Louarn, Jean-François Chailan

► **To cite this version:**

Sigrid Assengone Ootogo Be, Lénaïk Belec, Armand Fahs, Isabelle Martin, Guy Louarn, et al.. Impact of the sizing reactivity of glass fibers on composites hydrothermal aging. *Polymer Degradation and Stability*, 2023, 215, pp.110426. 10.1016/j.polymdegradstab.2023.110426 . hal-04182620

HAL Id: hal-04182620

<https://hal.science/hal-04182620>

Submitted on 29 Aug 2023

HAL is a multi-disciplinary open access archive for the deposit and dissemination of scientific research documents, whether they are published or not. The documents may come from teaching and research institutions in France or abroad, or from public or private research centers.

L'archive ouverte pluridisciplinaire **HAL**, est destinée au dépôt et à la diffusion de documents scientifiques de niveau recherche, publiés ou non, émanant des établissements d'enseignement et de recherche français ou étrangers, des laboratoires publics ou privés.

Impact of the sizing reactivity of glass fibers on composites hydrothermal aging

Sigrïd Assengone Otogo Be¹, L  naïk Belec¹, Armand Fahs¹, Isabelle Martin¹, Guy Louarn², Jean-Fran  ois Chailan¹

¹ Laboratoire MAPIEM, Universit   de Toulon, CS 60584, 83041 Toulon Cedex 9, France.

² Universit   de Nantes, CNRS, Institut des Mat  riaux Jean Rouxel, IMN, 2 Rue de la Houssini  re, 44000 Nantes, France.

Abstract

Epoxy composites were prepared with reactive and non-reactive sizings deposited on glass fibers. The resulting interphase properties have been studied during hydrothermal aging. The purpose here is to evaluate at nano and macroscale the dependence of aging, interfacial strength, and mechanical properties of model composites on the glass sizing reactivity. SEM/AFM, DMA and 3 points bending experiments have been done before and after water immersion at 70   C for several weeks. Water diffusion kinetics have been found to be related only to the presence of sized glass fibers but not to the sizing reactivity. The SEM observations demonstrated a cohesive fracture at matrix/fiber in the case of composite elaborated with reactive sizing and an adhesive one in the case of non-reactive sizing, and this remains true with aging. Depending on the sizing nature and on the aging time, the evolution of interphase zones around fibers has been identified by a specific α -relaxation ($\text{Tan } \delta$) and confirmed by AFM nanomechanical measurements. The results showed that the interphase thickness was almost the same at initial state (around 200 nm) for both composites, then it progresses with aging time to reach 400 nm and 500 nm (at 42 days) for reactive and non-reactive systems respectively. It suggests that

water molecules diffusion is related to the hydrophilic character of the sizing and to the degree of cross-linking/or plasticization of the interphase during hydrothermal aging.

Keywords

Epoxy composites; hydrothermal aging; sizing reactivity; interphase properties; glass fibers.

1 Introduction

Interfacial properties in fiber-reinforced polymers have a strong influence on initial mechanical properties and on their in-service life. The development of offshore wind or tidal turbines subjected to severe mechanical and environmental conditions subsequently has led our knowledge of the materials used to extend their durability. Glass fibers/epoxy composites are, by far, the most used systems to support wind turbine blade loads. Strong cohesive interfaces generally result in high stiffness and mechanical strength of the composite. Nevertheless, strong bonds can reduce the composite toughness and fatigue resistance. Soft bonds generally improve dynamic properties by promoting the energy dissipation through the interfacial area [1,2]. These properties can be achieved by choosing an appropriate fiber treatment which will impact the interfacial properties and as a result, the composite durability from a mechanical and environmental point of view [3–6]. A suitable coupling agent which forms stable chemical bonds between the matrix and the reinforcement can thus limit the water diffusion at the

interface and consequently, the impact on mechanical properties [7]. Characterizing the interphase regions is difficult due to its dimensions and to the various interactions between its components [8–10]. Numerous studies have shown the potential of dynamic mechanical analysis (DMA) to reveal interphases in composites [5,11–14]. Depending on fiber treatments and matrix nature, the main relaxation peak may be more or less enlarged or even split into distinct relaxations. Local measurements such as nano-indentation tests with diamond tips have been used for many years to characterize interphases in composites [15]. Nevertheless, the mechanically impacted areas are generally larger than those of the interphases, and artefacts due to fiber response systematically lead to interphases with higher stiffness than the matrix one [9,16–19]. The use of low forces limits these artefacts by decreasing the impacted area [17,20,21]. Based on this method, the PeakForce Quantitative Nanomechanical Mapping (QNM) AFM mode performs force curves below 50 nN at 2 kHz during the scan to reach resolutions compatible with interphase sizes. The analysis of each force separation curve gives modulus, adhesion or deformation scans simultaneously with topographic imaging [22–24]. The force modulation mode also provides information on the local elasticity of the sample surface using an oscillating lever that indents the sample surface. Interphases of 20-80 nm width in carbon fiber/epoxy system could be measured by this method [25]. To measure the interfacial strength, mechanical tests can be performed at different scales and in different loading directions according to fiber axis. Macroscopic tests on unidirectional composites in transverse direction emphasize the matrix and interphase response in tension compared to longitudinal tensile or bending tests where fiber response dominates. The impact of interfacial properties on hydro/hygrothermal aging of composites has been shown in many studies, mainly by standard mechanical tests [26-35]. A decrease in composites stiffness and strength is usually measured under static or dynamic loading [26,27]. The drop in mechanical properties can be twice higher for the composite laminates than for the neat resin subjected to the same conditions (immersion

at 50 °C for 200 days) [28]. In non-crimp basalt fiber/epoxy systems, the strength in flexural, interlaminar and in-plane-shear is decreased by 20 % after moisture aging [29]. Similar results were obtained by [30] after immersion in sea water at different temperatures of glass/epoxy and basalt/epoxy composites subjected to static and fatigue tests. E-glass/epoxy composite pipes immersed at different temperatures under compressive loads showed a decrease in burst pressure with increasing aging time, immersion temperature and pre-load due to debonding between fibers and matrix [31]. A cyclic hygrothermal aging performed between 30 °C and 60 °C with 95 % RH on woven glass fiber/epoxy laminates leads to a decrease of impact strength by 15 % due to the degradation of matrix and fiber/matrix interface and localization of the transverse deformation [32]. A comparative study of hygrothermal aging effects on low velocity impact strength was performed on carbon fiber and glass fiber reinforced epoxy composites [33]. After around 40 days of immersion at 80 °C, the impact properties of CFRP increased by 20 % in contrast to that of GFRP composites which decreased by 30 %. The difference was attributed to the degradation of glass fibers surface rather than to an interfacial degradation. [34] studied the tensile and short beam strength degradation of glass fiber /epoxy laminates immersed in a saline solution at different temperatures. The impact of the curing cycle and of the loading direction are analysed. High curing temperatures limit the strength degradation due to a higher bonding strength between fibers and matrix. The strength degradation is less for tensile test specimens compared to ILSS test specimens because fibers are less affected compared to matrix in hygrothermal environment. Depending on the environmental conditions, the nature of the filler may also impact differently the tensile properties of epoxy-amine composites [35]. The degradation of Young's modulus depends on wet conditions but is independent of the filler type. Conversely, the tensile strength is affected by the interfacial properties and depends notably on fillers reactivity.

These different studies show up the importance of fiber-matrix interfacial bonds on composites mechanical properties, especially in hydro/hydrothermal conditions. To better understand the influence of interfacial bond strength on mechanical properties in one hand and on hydrothermal resistance on the other hand, model epoxy composites with strong and soft interfacial bonds were developed by varying the reactivity of glass fibers sizing. Physico-chemical characterizations and mechanical measurements were performed on composites from nano to macroscale before and after immersion at 70 °C during several weeks.

2 Materials and methods

A reactive or non-reactive fiber treatment are designed to create cohesive or soft interphases respectively in glass fiber/epoxy systems. The reactive sizing consists of 3-aminopropyltrimethoxysilane coupling agent (APTMS) associated to a Bisphenol A diglycidyl ether-based epoxy DGEBA film former. The other one consists of a methyltriethoxysilane (MTES), non-reactive with the epoxy-amine matrix, associated to a neutralized DGEBA synthesized from DGEBA and diethylamine (DEA) using Makvandi et al. method [36] (Fig. 1). The resulting Bisphenol A glycerolate diethylamine or BGEA was analyzed by infrared spectroscopy using a Thermo-Nicolet is50 spectrometer to control the neutralization of oxirane groups [37].

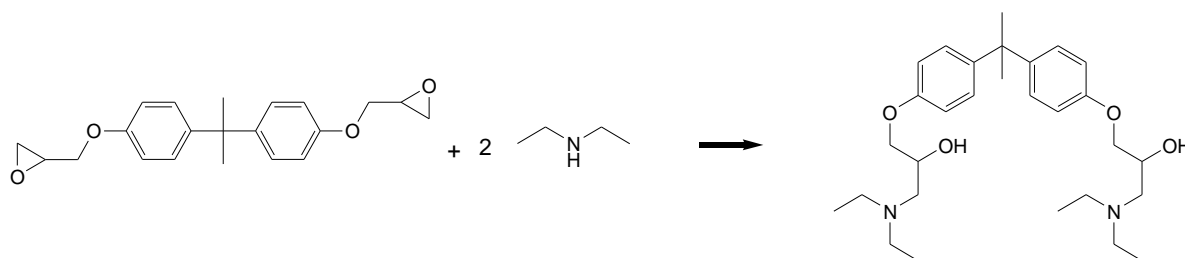


Fig. 1. Synthesis of BGEA film former (neutralized DGEBA) [36]

Before treatment, the E-glass fibers supplied by Owens Corning Reinforcement were placed in an acetone solution boiling at 56°C for 5 h, rinsed for 10 min with acetone and heated above

400 °C for 90 min to remove any residual organic compound from the surface. They were stored in a desiccator before use.

The APTMS and MTES silane solutions were prepared at a concentration of 1 wt% in ethanol. For the APTMS solution, a few drops of acetic acid were added to avoid condensation. The cleaned glass fibers were immersed in the APTMS or MTES solutions for 1 h at room temperature, rinsed with ethanol and heated 30 min at 110°C in the oven followed by an overnight condensation reaction at room temperature. APTMS and MTES silane-grafted fibers were immersed for 20 min. in film-forming solutions of DGEBA and BGEA respectively, at a concentration of 0.005 mol L⁻¹ in acetone. The glass fibers were then removed and dried overnight in an oven at 60 °C.

The epoxy resin and matrix of the composites are based on a DGEBA prepolymer with $n = 0.15$ supplied by Sigma Aldrich under the reference 31185. This compound was also used as the reactive film former and as the base for BGEA synthesis. An aliphatic amine was chosen as cross linker, the diethylenetriamine (DETA, supplied by Acros Organics), for its common use in industry, its low molecular weight and good reactivity. The prepolymer and hardener were mixed at a DGEBA/DETA ratio of 10/1.09 by mass to be in stoichiometric proportion. For reinforced composites, the mass ratios of DGEBA/glass/DETA were 10/4.75/1.09. The unidirectional composites were moulded with 25^{±4} wt% of sized fibers and cured during 2 h at 60 °C followed by 2 h at 120 °C and 4 h at 130 °C. The same curing cycle is used for resin plates. Fibers are randomly distributed into the matrix and no porosity was observed by SEM (see Fig.S1 in supplementary information).

Hydrothermal aging was performed by immersion at 70 °C up to 120 days in deionized water. The kinetics of water diffusion were determined from gravimetric measurements on plates of 49 x 27 x 2 mm³ with fibers displayed longitudinally and edges protected to avoid fiber/matrix

preferential water diffusion pathways. Measurements were performed on 3 distinct samples for repeatability. To control the reversibility of water effects, samples immersed for 42 days were desorbed in a vacuum oven at 50 °C up to mass stabilisation which was reached around 40 days.

The evolution of the interfacial strength was characterized in each case by 3 points transverse bending according to ISO 178 on a INSTRON testing device. Microfractography of the composite materials was performed on a scanning electron microscopy (Zeiss-Supra 40 VP/Gemini Column) in secondary electron mode. The samples were coated with thin layer of carbon under vacuum before SEM imaging.

XPS experiments were done on Kratos Nova spectrometer to determine the surface chemical compositions of the glass fibers on 300 μm \times 700 μm areas. Binding energy was collected in the range of 0-700 eV. The surface chemical composition was determined using integrated peak areas using CasaXPS software.

Nanomechanical characterization of composites interphases was done on a Multimode 8 microscope from Bruker using the PeakForce Quantitative Nano-Mechanics mode (PF-QNM). Force curves were obtained at 2 kHz with a setpoint force around 20 nN, to limit the deformation of sample surface below 2 nm. Several calibration steps are required on reference samples to get the cantilever stiffness and the tip radius of the probe which enable DMT modulus measurements. The cross-sections of composites for nanomechanical measurements were successively polished with diamond suspensions and alumina oxide suspensions to 0.04 μm . The surfaces were then cleaned with water and finally dried with air before each measurement.

Dynamic Mechanical Analysis (DMA) was operated on a Q800 from TA Instruments in single cantilever mode. Composite samples of 40 x 25 x 2 mm³ were cut in transverse direction to fiber axis to amplify the interphase response. Experiments were performed at a heating rate of

3 °C/min with an amplitude of 20 μm at a frequency of 1 Hz. The damping peak associated to the α-relaxation was analysed and deconvoluted by Origin® using a Gaussian model. Cumulated errors resulting from samples dispersion and deconvolution method give a standard deviation of +/- 3 °C.

3 Results and discussion

3.1 Before aging

The cleaning process and SEM/AFM observations of fibers were presented in a previous study [37]. The chemical analysis of sized fibers by XPS confirms the presence of organic compounds. The first step consisting in grafting APTMS and MTES silanes succeeded if we consider the increase in carbon amount in both cases and the presence of nitrogen in the case of APTMS. After DGEBA film former deposition, the amount of nitrogen is slightly decreased due to the higher proportion of carbon from DGEBA. Silicon rate is lower but still present revealing a thin or inhomogeneous film deposition. In the case of MTES-BGEA treated glass fibers, the amount of nitrogen and carbon are logically higher due to oxirane neutralization by DEA. The important decrease of glass components (Si, Ca) confirms the deposition of a thick organic layer in that case.

Table 1. Relative atomic proportion (%) obtained by XPS analysis of untreated and treated glass fibers. * Presence of atmospheric contaminant

Sample	C	O	N	Si	Ca
Cleaned surface	*	68.1	0	25.6	6.3
APTMS	29.8	45.2	2.8	18.4	3.8
MTES	13.7	62.2	0	21.5	2.6
APTMS + DGEBA	26.6	48.1	2.0	19.1	4.2

MTES + BGEA	54.4	29.3	3.7	10.2	2.4
--------------------	------	------	-----	------	-----

The sizing present on fibers can interact with the matrix network during the impregnation and subsequent curing process [16,38]. Plasticizing effects or crosslinking modifications around fibers will modify the mobility and then impact the damping peak obtained by DMA [11–13]. In the case of the viscoelastic response of the resin alone, a small shoulder at lower temperature (around 120 °C) is visible. It is attributed to an imperfect crosslinking despite curing cycle optimization. The whole peak is deconvoluted considering Gaussian peaks. The ratio in terms of peak surface between the under-crosslinked network and the homogeneous matrix is around 2 % (Fig. 2). As for the pure resin, a shoulder at low temperature is also visible on the DMA relaxation peak for both composite systems (Table 2). From deconvolution analysis, the relaxation at low temperature takes place respectively 9 °C and 6 °C higher for APTMS-DGEBA and MTES-BGEA composites than for the resin. Moreover, the peak surface ratios for the APTMS-DGEBA and MTES-BGEA systems represent more than 6 % and 4 % respectively. The comparison with the resin behavior is consequently attributed to the presence of treated fibers which impacts the matrix network around fibers.

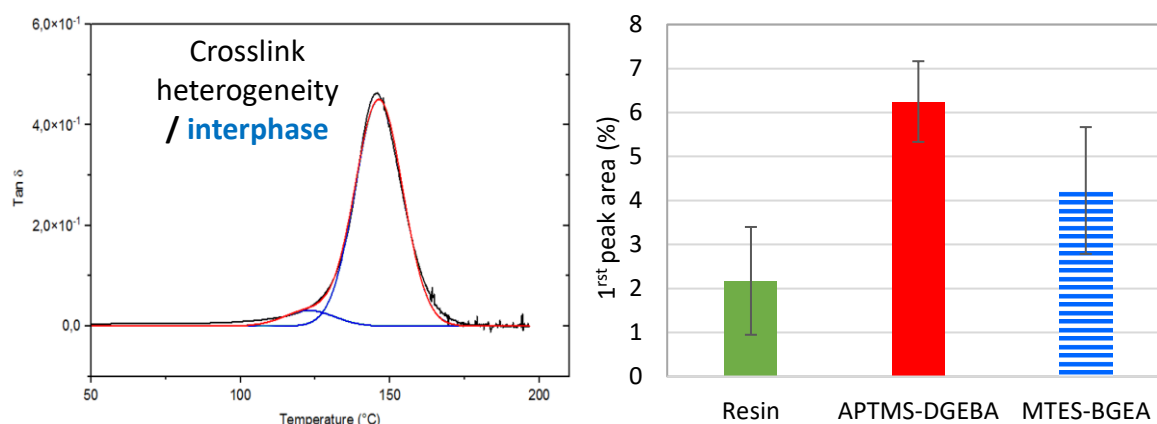


Fig. 2. DMA relaxation peak ($\text{Tan } \delta$) deconvolution and comparison of the first peak proportional area for the resin and for the composites reinforced with APTMS-DGEBA and MTES-BGEA sized fibers.

Table 2. Thermomechanical data for the resin and composites at initial time (DMA, 1 Hz, 20 μm , 3 $^{\circ}\text{C}/\text{min}$).

Resin		EP-F-APTMS-DGEBA		EP-F-MTES-BGEA	
$\text{T}\alpha_{(\text{heterogen})}$	$\text{T}\alpha$	$\text{T}\alpha_{(\text{int})}$	$\text{T}\alpha_{(\text{dry})}$	$\text{T}\alpha_{(\text{int})}$	$\text{T}\alpha_{(\text{dry})}$
121	154	130	149	127	152

APTMS-DGEBA reactive system presents an excess of oxirane groups due to DGEBA film former deposited on fibers. This excess modified the stoichiometry near the fibers when they are incorporated in the matrix during the impregnation and curing process. This off-stoichiometry can generate a crosslinking gradient corresponding to the interphase around fibers. For the MTES-BGEA system, non-reactive BGEA molecules are present near the fiber surface and can diffuse into the resin during the elaboration. It can consequently plasticize the network without modifying the epoxy/amine stoichiometry around fibers. The network in that case may consequently be correctly crosslinked but just plasticized, leading to an intermediate peak proportional area of only 4 % compared to 6 % for the reactive system.

The sizing impacts the network around fibers as shown by DMA relaxation peak analysis. To show up the impact on interfacial strength, composite samples were fractured, and the surfaces were analyzed by SEM (Fig.3). The fractured surfaces reveal very different failure modes depending on sizing nature. The reactive system with APTMS-DGEBA sizing generates a cohesive failure mode with adherent matrix recovering fibers, while the non-reactive system with MTES-BGEA sizing leads to an adhesive failure at fiber/matrix interface.

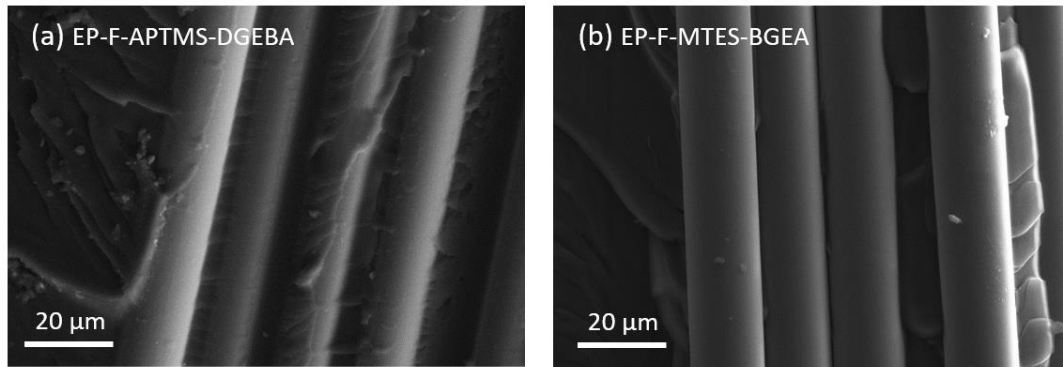


Fig.3. SEM microfractography of composites reinforced with (a) APTMS-DGEBA sized fibers and (b) MTES-BGEA sized fibers.

It was shown in a previous study [37] that these model interphases between E-glass fibers and epoxy resin could be correlated to the interfacial strength and to the mechanical properties of the composites from nano to macroscale. DMA confirms the existence of a network with increased molecular mobility compared to the bulk matrix which depends on sizing chemistry. It seems essential to try and correlate the impact of these model interphases on hydrothermal aging.

3.2 During hydrothermal aging

3.2.1 Impact of sized fibers on water absorption

The kinetics of water absorption are different between the resin and the composites (Fig.4). For the resin, a pseudo plateau is reached around $29 \text{ h}^{1/2}$ (35 days) but the water uptake increases again up to 120 days. For composites, saturation at 2.3 wt% is reached at 40 days. No impact of fiber treatment is clearly shown. The stabilisation suggests that no degradation nor interfacial decohesion take place during the whole period of immersion. Longer aging times could discriminate the water effects between both composite systems.

Considering that only the matrix absorbs water and using the resin absorption kinetics, a simple mixture law is used to calculate the theoretical water absorption of composites (equation 1). No

barrier effect resulting from fiber presence is observed. On the contrary, after 1 week of immersion, the experimental water absorption for composites is higher than the calculated one. The trend is likely to be reversed above 120 days of immersion. The water diffusion kinetic within the composites is consequently different from the resin one. The DGEBA/DETA stoichiometry and the curing cycle being the same for the composites and for the resin, it suggests that the sized fibers modified the matrix network during the composite elaboration.

$$M_{co}^{theo} = M_{re}^{exp} \times (1 - \Phi_f^m) \quad \text{Equation 1}$$

with a fiber fraction Φ_f^m of $25^{\pm 4}$ wt%.

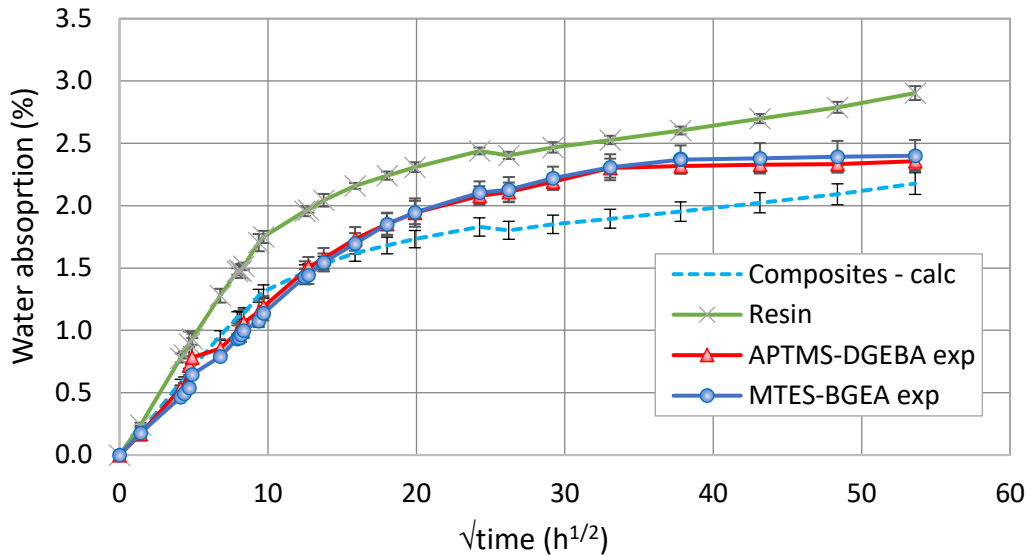


Fig.4. Water uptake of the resin and composites during immersion at 70 °C in deionized water compared with theoretical absorption.

3.2.2 Impact of hydrothermal aging on interphases

During aging, the viscoelastic response of the resin clearly differs from that of the composites (Fig.5). Indeed, the relaxation can be deconvoluted into 3 successive relaxations for both composite systems for all aging times, instead of 2 relaxations for the resin. It should be noted that the relaxation at low temperature of the resin is attributed to the network plasticized or degraded by water at longer immersion times. This phenomenon is classically observed during

immersion [39]. The additional relaxation peak at low temperature for the composites is around 15 degrees lower than the 1st peak of the resin, whatever the immersion time (**Erreur ! Source du renvoi introuvable.3**).

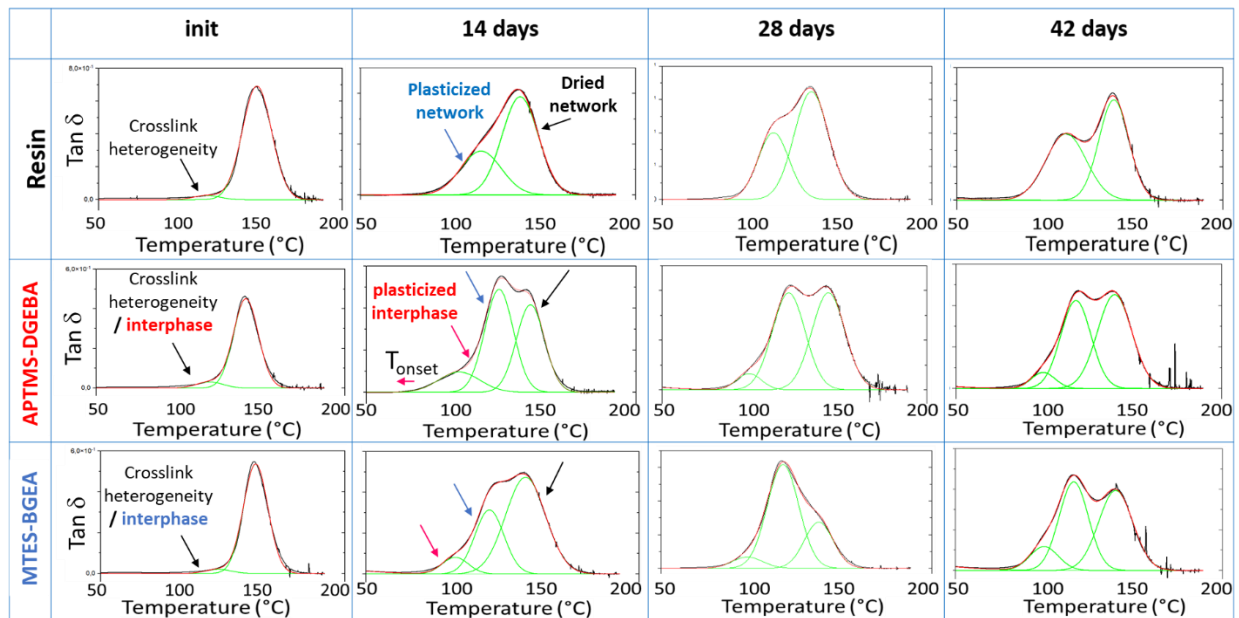


Fig.5. DMA α -relaxation peak ($\text{Tan } \delta$) with a Gaussian model deconvolution for the resin and the composites

This additional peak with a T_{α} centered around 102 °C is consequently attributed to the relaxation of the interphase plasticized by water. The 2nd peak is respectively around 125 °C for APTMS-DGEBA and 122 °C for MTES-BGEA (Table 3). This difference is not significant considering the standard deviation (3 °C) resulting from the deconvolution method. This 2nd peak is attributed to the plasticized matrix. Indeed, it is similar in terms of amplitude and temperature to the peak attributed to the plasticized resin. The relaxation above 145 °C is finally attributed to the dry network and/or to the network potentially dried during DMA heating experiment at 3 °C/min [39]. This latter peak shows a maximum which remains lower than the initial T_{α} , suggesting that the network is not completely dried or that it is degraded with aging times. The water absorption kinetics are similar for both systems (Fig.4), however the evolution of the respective peak areas and relaxation temperatures are different during aging (Fig.6 and

Table 3). After 14 days of immersion, the $T\alpha$ and the peak area of the interphase plasticized by water (Fig.6 a) are lower for the non-reactive MTES-BGEA system than for the reactive one. The peak areas of the plasticized interphase of the reactive and non-reactive systems represent respectively 14 % and 7 % of the whole relaxation peak. In the non-reactive system, the presence of unbound BGEA molecules that occupy free volumes around fibers can delay the arrival of water molecules within the interphase. The water absorption kinetics being similar for both composites, it suggests that water molecules preferentially diffuse into the interphase for the reactive system and into the whole matrix for the unreactive one up to 28 days of immersion. This is confirmed by the intensity of the 2nd peak which is attributed to plasticized matrix. This last is indeed higher for the MTES-BGEA system than for the APTMS-DGEBA system after 14 and 28 days of immersion (Fig.6 b).

Between 14 and 28 days, a huge decrease of the plasticized interphase peak area is observed for the reactive system. In the meantime, a continuous increase of the interphase peak takes place for the unreactive system up to 42 days of immersion. The interphase peak area reaches 11 % for the MTES-BGEA system while it is stabilized at around 6 % for APTMS-DGEBA system (Fig.6a). A contrary evolution is observed on the 2nd peak attributed to the plasticized matrix between 28 and 42 days, especially for the non-reactive system. It suggests that water molecules are transferred from the plasticized matrix to the interphase without changing the whole amount of water in composites.

Table 3. Thermomechanical data for the resin and composites during hydrothermal aging (DMA, 1 Hz, 20 μ m, 3 °C/min).

Sample	Resin		EP-F-APTMS-DGEBA			EP-F-MTES-BGEA		
	$T\alpha_{(plast)}$	$T\alpha_{(dry)}$	$T\alpha_{(int)}$	$T\alpha_{(plast)}$	$T\alpha_{(dry)}$	$T\alpha_{(int)}$	$T\alpha_{(plast)}$	$T\alpha_{(dry)}$
14 days	120	143	105	127	147	102	122	144
28 days	116	138	103	126	150	101	122	143

42 days	116	144	103	122	145	103	121	146
----------------	-----	-----	-----	-----	-----	-----	-----	-----

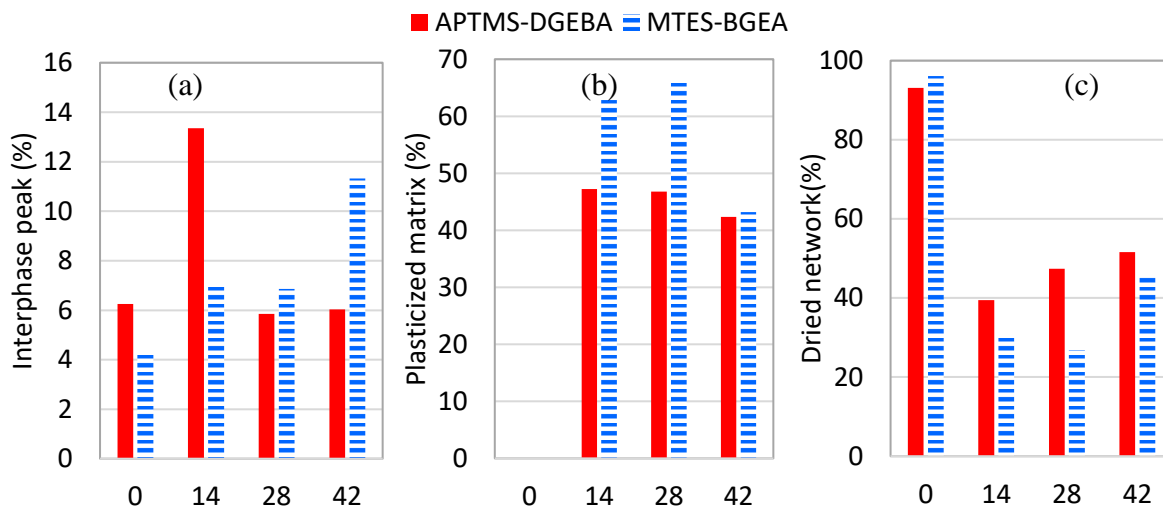


Fig.6. Evolution of the areas (%) of the different peaks obtained for the deconvoluted α -relaxation as a function of aging time (in days). (a) plasticized interphase, (b) plasticized matrix, (c) dried network.

The results are supported by the analysis of dynamic modulus. A decrease of the elastic modulus is observed during the hydrothermal ageing due to the plasticization of the epoxy network (Fig. S2).

To confirm the presence of interphases around fibers and to characterize their evolution during hydrothermal aging, nanomechanical measurements were performed on polished UD composites in transverse mode.

Fig.7 shows the nanomechanical maps of the model composites. These are representative examples of many PeakForce QNM analyses over several regions around the fibers. The darker areas on the maps correspond to lower modulus values. These areas seem to be preferentially located in the vicinity of the fibers and are heterogeneously distributed. This observation can be correlated to the heterogeneity of the sizing distribution during deposition as observed in a former study [37]. These zones, which present different mechanical properties from those of the matrix, correspond to the interphase detected by the deconvolution method in DMA.

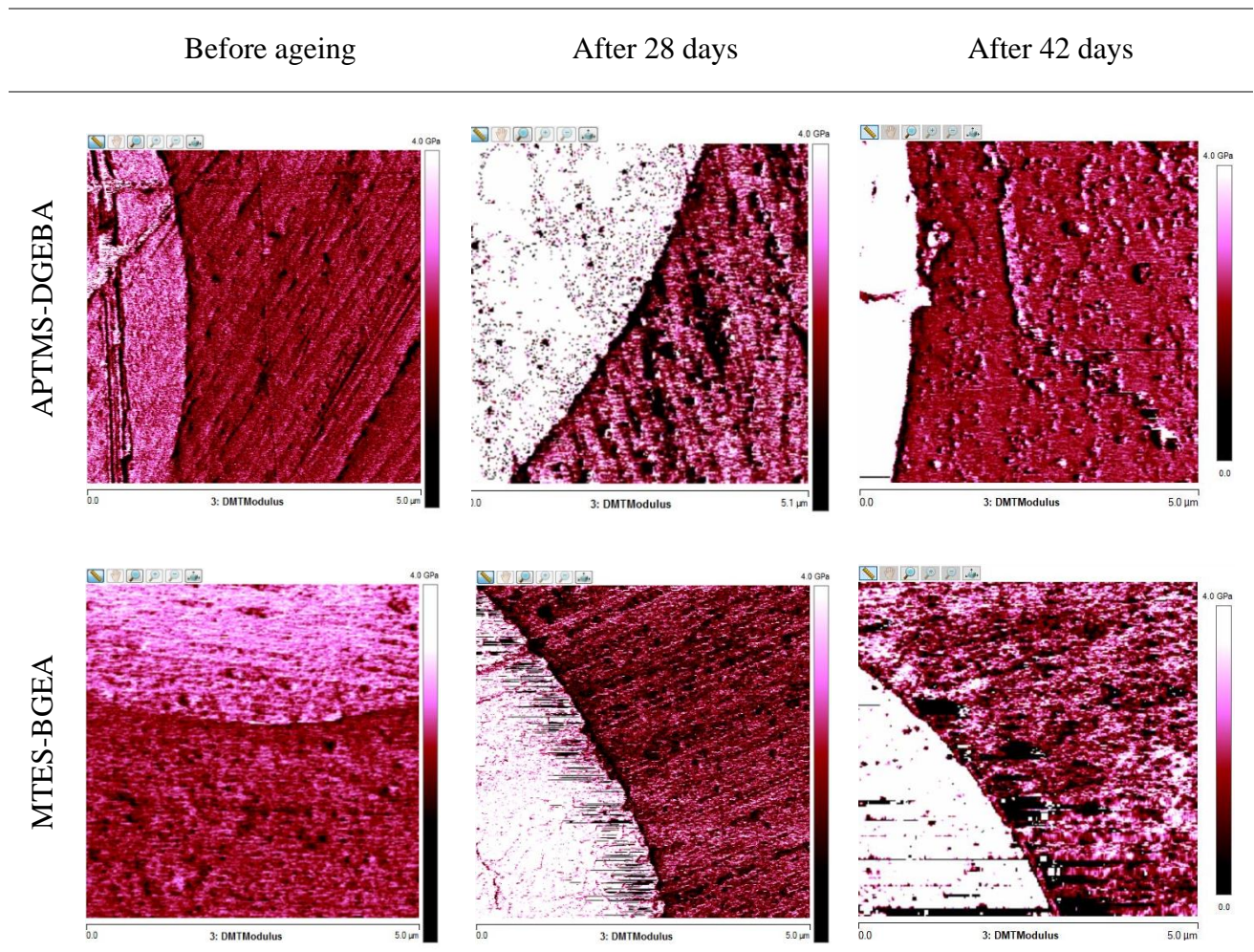
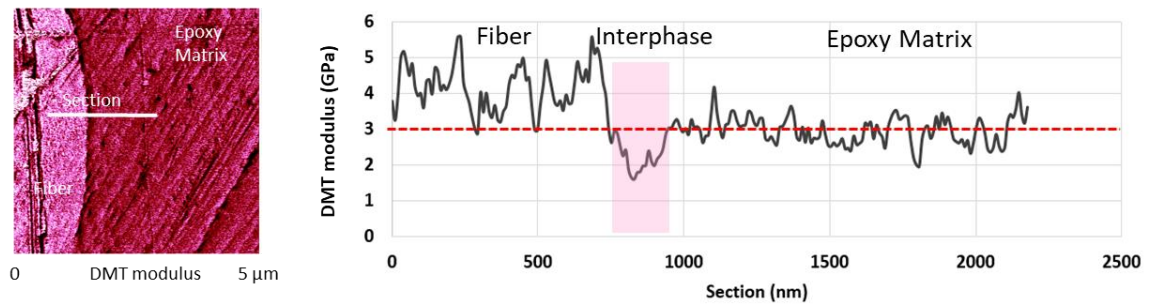


Fig.7. DMT modulus maps (5 μm) of the composites before and after hydrothermal aging at 28 and 42 days.

To estimate their average thickness, cross-sectional profiles were taken on the nanomechanical maps for all systems at initial time t_0 and during aging (Fig.8). The mean DMT modulus value of the matrix is represented by a horizontal dash line which is superimposed to profiles. The interphase is defined by the area around fibers where modulus values are below this line, i.e. lower than the matrix mean value.

(a) EP-F-APTMS-DGEBA - initial



(b) EP-F-APTMS-DGEBA after 42 days

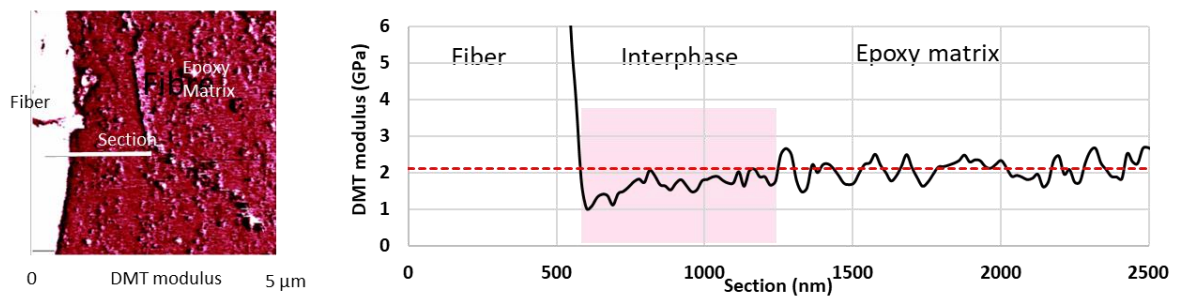


Fig.8. Example of DMT modulus profiles obtained for the EP-F-APTMS-DGEBA composite at initial time and after 42 days of hydrothermal aging.

The interphase thicknesses were measured on 10 profiles by this method. **Fig.9** shows the evolution of the interphase thickness as a function of aging for the reactive and non-reactive composite systems. At initial time, the average thicknesses are around 200 nm.

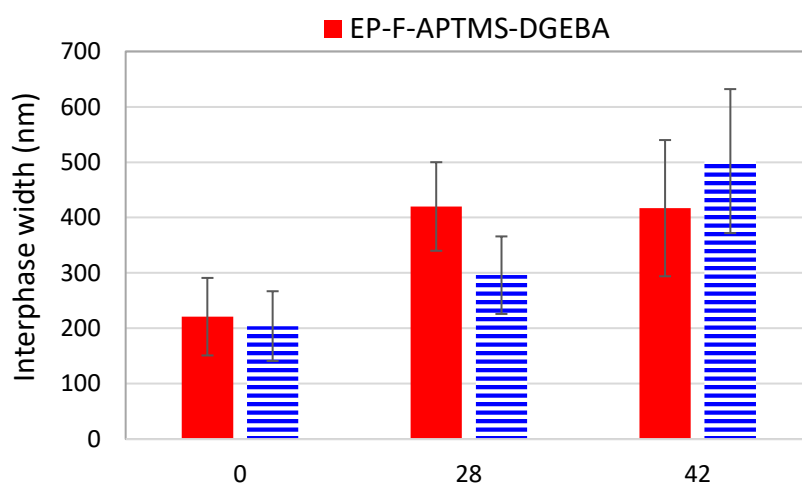


Fig.9. Evolution of the interphase width of model composites as a function of aging time (days).

During aging, the thickness of the interphases increases for both systems, up to approximately 500 nm for the EP-F-MTES-BGEA non-reactive system and to 420 nm for the reactive EP-F-APTMS-DGEBA system after 42 days of immersion. The main difference is observed after 28 days of aging where the interphase width of the reactive system has already reached its maximum value (420 nm) while it is only 300 nm width for the non-reactive one. The effects of water on interphase properties are consequently delayed in that case. The reactive interphase is under-crosslinked and more hydrophilic due to the excess of oxirane groups around glass fibers. Water molecules can then be stored inside the interphase before saturating the matrix. This leads to a more rapid increase of interphase thickness for the reactive system than for the non-reactive one.

Beyond 28 days, water molecules diffuse into the matrix and no longer modify the interphase, as has been demonstrated in DMA study. In the case of the non-reactive system, a progressive increase in interphase thickness is observed, which is also consistent with the DMA tests.

3.2.3 Impact of glass sizing on interfacial strength during hydrothermal aging

To show the influence of fiber treatment on the evolution of interfacial strength during aging, 3 points bending tests were performed in transverse mode on model composites. In that direction, fibers do not contribute to the mechanical strengthening of the composite. The fiber/matrix interfacial response is amplified, which should impact the strain and stress at break and discriminate both systems. The bending modulus mainly reflects the elastic response of the matrix and to a lesser extent that of the interphase.

While the water absorption kinetics are similar throughout the whole aging period for both model composites, the evolution of elastic properties and data at break are different according to sizing reactivity (Fig.10). The bending modulus of EP-F-APTMS-DGEBA composite decreases gradually and is nearly divided by 2 after 42 days of immersion while it is barely

affected for the non-reactive EP-F-MTES-BGEA system. Considering data at break, they increase after 14 days of immersion due to the matrix and interphase plasticizing. Beyond that time, the stress and strain at break decrease, especially for the non-reactive system after 28 days of immersion. The mean value for the stress at break is only 40 MPa for the EP-F-MTES-BGEA system compared to 62 MPa for the EP-F-APTMS-DGEBA system after 28 days of aging. The load transfer between the matrix and the fiber is consequently more affected by water for the EP-F-MTES-BGEA composite system. The differences observed between elastic properties and data at break have already been reported in epoxy-fillers composites [35]. The fillers reactivity impacts the tensile strength during aging while elastic properties are independent on filler nature in humid conditions.

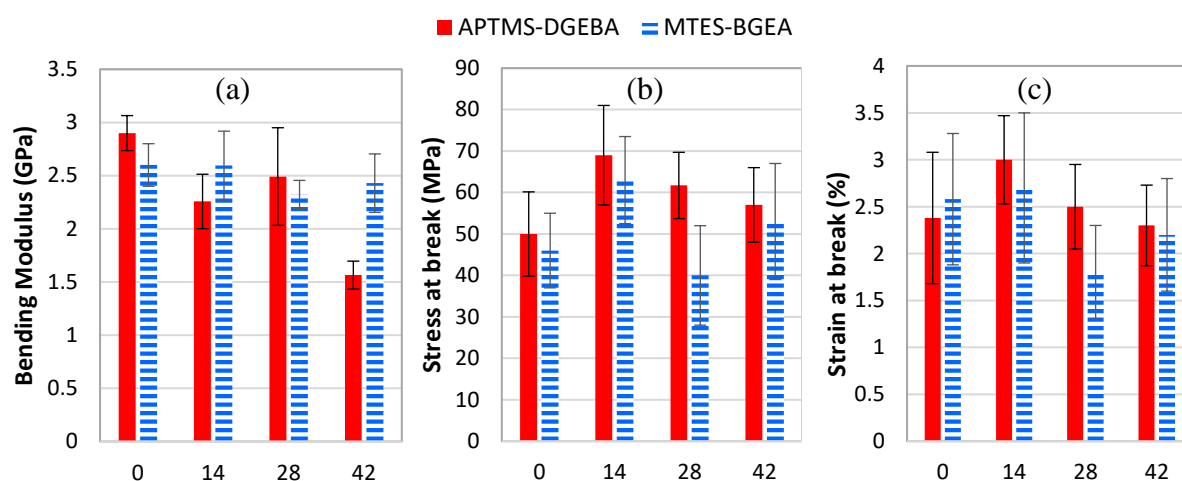


Fig.10. Impact of aging on 3-points bending properties. (a) Bending modulus, (b) Stress at break (MPa), (c) Strain at break (%).

To understand the differences observed after 28 days of immersion between both systems in terms of bending strength, microfractography was performed by SEM on fractured samples (**Fig.11**). The fracture is still mainly cohesive for the EP-F-APTMS-DGEBA reactive system with matrix still adherent to fiber surface, while the facies is adhesive at matrix/fiber interface for the non-reactive EP-F-MTES-BGEA composite. Moreover, many fragments are visible on the fractured surface. The differences observed can explain the lower interfacial strength obtained for the EP-F-MTES-BGEA composite system compared to the reactive one.

This result shows that fiber treatment is more impactful on degradation than fiber hydrolysis as suggested by some authors [40,41]. In case of a predominant fiber hydrolysis mechanism, a similar fracture mode would be observed on both systems. In our case, fiber surface remains smooth after the adhesive fracture up to 28 days. Above 28 days the hydrolysis of fibers may also be possible.

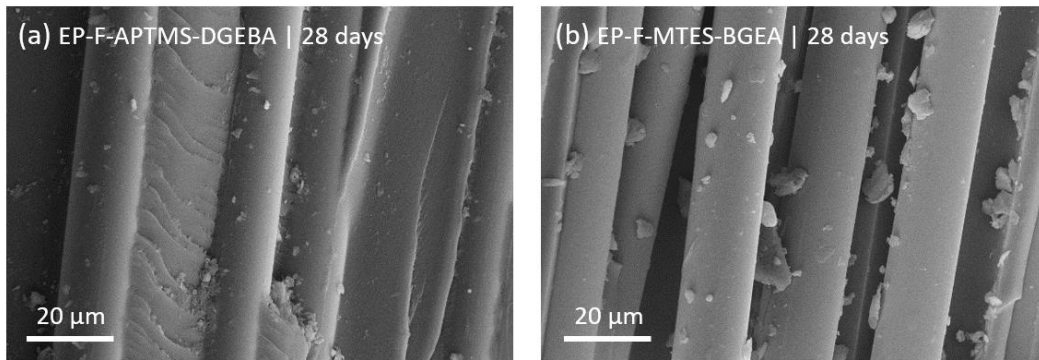


Fig.11. SEM microfractography of composites reinforced with (a) APTMS-DGEBA sized fibers and (b) MTES-BGEA sized fibers after 28 days of hydrothermal aging.

Differences in terms of interphase evolution and interfacial strength are shown during aging according to the reactivity of the fiber treatment. The water molecules will not be distributed in a similar way inside the matrix or in the interfacial area during immersion. To highlight the effects of water during hydrothermal aging on both model composites and on the resin alone, the samples were dried after 42 days of aging and characterized again.

3.3 Reversibility of the effects

To study the reversibility of the effect of hydrothermal aging on the resin and model composites, DMA experiments were performed on samples dried after 42 days of immersion. The Fig.12 shows the relaxation of the dried resin after 42 days of aging. The main relaxation is shifted by -9°C compared to the initial resin and a large shoulder is present around 100°C . The relaxation at low temperatures represents 14 % of the overall peak area compared to 2 % for the resin at

initial state. It reveals irreversible modifications of the network after 42 days of immersion at 70 °C such as hydrolysis of the network.

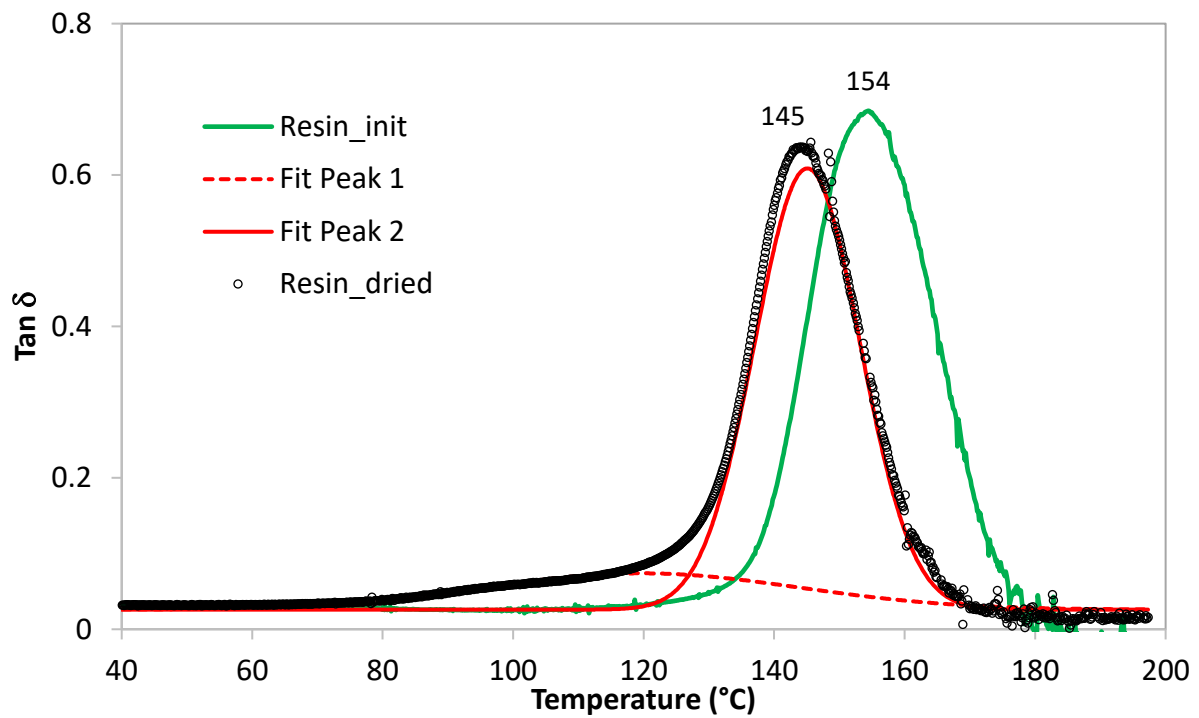


Fig.12. Tan δ obtained by DMA analysis of the resin at initial state and dried after 42 days of immersion at 70 °C and deconvolution of Tan δ of the dried resin.

Concerning model composites, the main relaxation peak after desorption is also shifted towards low temperatures for both systems. The shift is more pronounced for the EP-F-APTMS-

DGEBA composite with -9 °C compared to -2 °C for EP-F-MTES-BGEA composite (

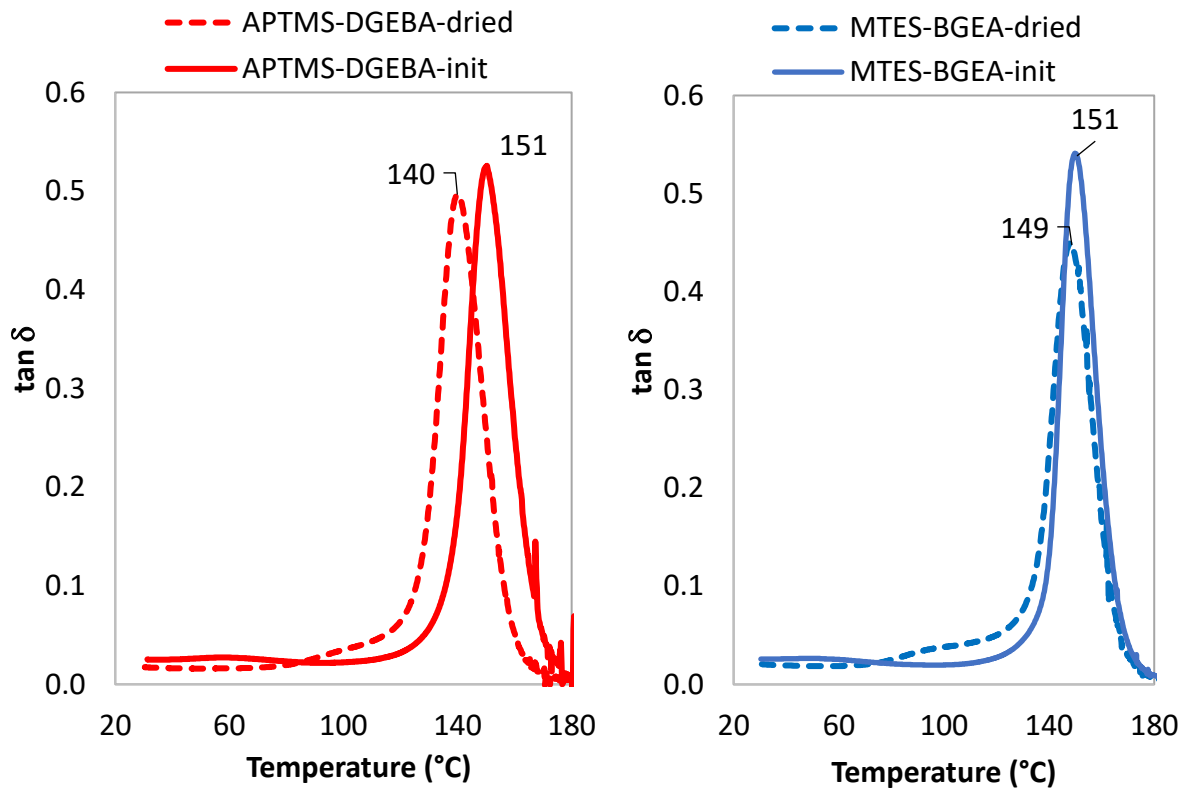


Fig.13). It can be noted that the reactive system was also more impacted than the non-reactive one after 42 days of immersion in terms of elastic properties (Fig.10). Furthermore, the shift is similar to that measured for the resin alone after desorption. In the case of the reactive EP-F-APTMS-DGEBA system, the degradation process of the matrix seems to be similar as the resin one. For the non-reactive EP-F-MTES-BGEA composite, the impact of water on the matrix could be delayed after 42 days, as shown by the elastic bending properties.

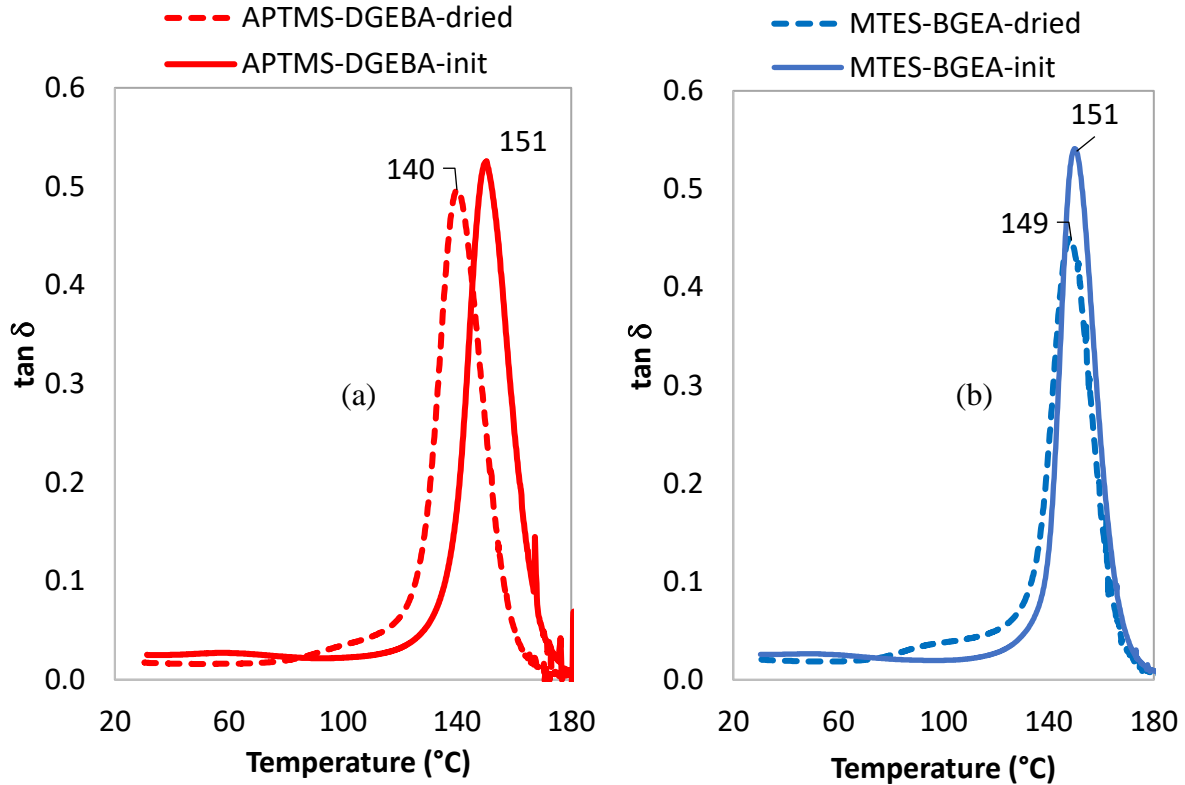


Fig.13. Evolution of the main relaxation for the reactive (a) and non-reactive (b) systems at initial time and dried after 42 days of immersion.

The relaxation peaks were deconvoluted for the systems, and the results were compared to that performed on the resin after desorption. The peak area, corresponding to the low-temperature shoulder, also represents between 14 and 15% of the overall relaxation area for the two systems, as in the case of the resin. This shoulder suggests a degradation related to the matrix and not specifically to the interphases.

4 Conclusion

Model composites with controlled interphases are elaborated and characterized under hydrothermal aging conditions. XPS analysis and microfractography show that the reactive APTMS-DGEBA sizing is successfully grafted to fibers and forms bonds with the epoxy matrix, while the non-reactive MTES-BGEA deposited on fibers results in a poor interfacial adhesion with the epoxy matrix. The water diffusion kinetics are influenced by the presence of

treated fibers but not by the nature of fiber treatment, at least for the fiber rates and aging times considered in our study. The interphases formed around fibers are highlighted by DMA which shows a specific α -relaxation, and by AFM nanomechanical measurements which enable the determination and the evolution of interphase thickness during aging. This last depends on the reactivity of fiber treatments. The differences observed in terms of interphase thickness and $\tan \delta$ area were attributed to the hydrophilic properties of the sizing and to the degree of cross-linking/or plasticization of the interphases (excess of oxirane for the reactive sizing and presence of unbound BGEA molecules for the non-reactive sizing). Water molecules diffuse preferentially in the reactive APTMS-DGEBA interphase than in the matrix for short aging times. In the case of composite with non-reactive sizing, water diffusion may be hindered by the free BGEA molecules present inside the interphase, so that water molecules first saturate the matrix. For longer aging times, corresponding to the Fickien plateau, the opposite phenomenon takes place. Water molecules diffuse from the interphase to the matrix for the reactive system and the interphase of the non-reactive systems progressively fills up.

Transverse bending gives the elastic response of the matrix and the interfacial strength during aging. The modulus is more impacted for the EP-F-APTMS-DBEBA system at 42 days than for the EP-F-MTES-BGEA system. The bending strength is oppositely and logically higher for the reactive system where the fracture mode is still cohesive after 28 days of immersion, while the non-reactive presented mainly adhesive at matrix/fiber interface from the beginning.

The reversibility study showed the hydrolysis of the resin and composites after 42 days of aging, especially for the EP-F-APTMS-DGEBA system. All systems show a broad shoulder at low temperature characteristic of network degradation.

In conclusion, the reactive sizing system is able to protect the fiber/matrix interface in the presence of water for these aging times. The non-reactive system weakens the interface but also

delays matrix hydrolysis. Composites with controlled interphases can then be developed according to the application. Moreover, the methods developed at multiscale can be used to optimize the elaboration of new composites such as bio-based composites where hydrothermal resistance must be improved.

Acknowledgments

The authors acknowledge the financial support ANBG (Agence Nationale des Bourses du Gabon).

References

- [1] M. Bar, R. Alagirusamy, A. Das, P. Ouagne, Low velocity impact response of flax/polypropylene hybrid roving based woven fabric composites: Where does it stand with respect to GRPC?, *Polym. Test.* 89 (2020) 106565. <https://doi.org/10.1016/j.polymertesting.2020.106565>.
- [2] N. Ranganathan, K. Oksman, S.K. Nayak, M. Sain, Impact toughness, viscoelastic behavior, and morphology of polypropylene-jute-viscose hybrid composites, *J. Appl. Polym. Sci.* 133 (2016) n/a-n/a. <https://doi.org/10.1002/app.42981>.
- [3] Y. Joliff, L. Belec, M.B. Heman, J.F. Chailan, Experimental, analytical and numerical study of water diffusion in unidirectional composite materials – Interphase impact, *Comput. Mater. Sci.* 64 (2012) 141–145. <https://doi.org/10.1016/j.commatsci.2012.05.029>.
- [4] Y. Joliff, W. Rekik, L. Belec, J.F. Chailan, Study of the moisture/stress effects on glass fiber/epoxy composite and the impact of the interphase area, *Compos. Struct.* 108 (2014) 876–885. <https://doi.org/10.1016/j.compstruct.2013.10.001>.
- [5] L. Belec, T.H. Nguyen, D.L. Nguyen, J.F. Chailan, Comparative effects of humid tropical weathering and artificial ageing on a model composite properties from nano- to macro-scale, *Compos. Part Appl. Sci. Manuf.* 68 (2015) 235–241. <https://doi.org/10.1016/j.compositesa.2014.09.028>.
- [6] L. Riaño, L. Belec, J.-F. Chailan, Y. Joliff, Effect of interphase region on the elastic behavior of unidirectional glass-fiber/epoxy composites, *Compos. Struct.* 198 (2018) 109–116. <https://doi.org/10.1016/j.compstruct.2018.05.039>.
- [7] D.L. Angst, G.W. Simmons, Moisture absorption characteristics of organosiloxane self-assembled monolayers, *Langmuir.* 7 (1991) 2236–2242. <https://doi.org/10.1021/la00058a043>.
- [8] X. Gao, R.E. Jensen, S.H. McKnight, J.W. Gillespie, Effect of colloidal silica on the strength and energy absorption of glass fiber/epoxy interphases, *Compos. Part Appl. Sci. Manuf.* 42 (2011) 1738–1747. <https://doi.org/10.1016/j.compositesa.2011.07.029>.
- [9] S.-L. Gao, E. Mäder, Characterisation of interphase nanoscale property variations in glass reinforced polypropylene and epoxy resin composites, (2002) 18.
- [10] R. Jensen, S. Mcknight, Inorganic–organic fiber sizings for enhanced energy absorption in glass fiber-reinforced composites intended for structural applications, *Compos. Sci. Technol.* 66 (2006) 509–521. <https://doi.org/10.1016/j.compscitech.2005.06.004>.

- [11] J.L. Thomason, Investigation of composite interphase using dynamic mechanical analysis: Artifacts and reality, *Polym. Compos.* 11 (1990) 105–113. <https://doi.org/10.1002/pc.750110206>.
- [12] J. Thomason, A note on the investigation of the composite interphase by means of thermal analysis, *Compos. Sci. Technol.* 44 (1992) 87–90. [https://doi.org/10.1016/0266-3538\(92\)90028-2](https://doi.org/10.1016/0266-3538(92)90028-2).
- [13] S. Keusch, R. Haessler, Influence of surface treatment of glass fibers on the dynamic mechanical properties of epoxy resin composites, *Compos. Part Appl. Sci. Manuf.* 30 (1999) 997–1002. [https://doi.org/10.1016/S1359-835X\(99\)00007-X](https://doi.org/10.1016/S1359-835X(99)00007-X).
- [14] S. Mallarino, J.F. Chailan, J.L. Vernet, Sizing effects on main relaxation process of cyanate ester glass fiber composites using dynamic mechanical and microthermal analyses, *J. Polym. Sci. Part B Polym. Phys.* 44 (2006) 205–214. <https://doi.org/10.1002/polb.20685>.
- [15] M.R. VanLandingham, R.R. Dagastine, R.F. Eduljee, R.L. McCullough, J.W. Gillespie, Characterization of nanoscale property variations in polymer composite systems: 1. Experimental results, *Compos. Part Appl. Sci. Manuf.* 30 (1999) 75–83. [https://doi.org/10.1016/S1359-835X\(98\)00098-0](https://doi.org/10.1016/S1359-835X(98)00098-0).
- [16] W.M. Cross, W.M. Cross, L. Kjerengtroen, J.J. Kellar, Interphase variation in silane-treated glass-fiber-reinforced epoxy composites, *J. Adhes. Sci. Technol.* 19 (2005) 279–290. <https://doi.org/10.1163/1568561054352649>.
- [17] A. Hodzic, Z.H. Stachurski, J.K. Kim, Nano-indentation of polymer–glass interfaces Part I. Experimental and mechanical analysis, *Polymer.* 41 (2000) 6895–6905. [https://doi.org/10.1016/S0032-3861\(01\)00029-5](https://doi.org/10.1016/S0032-3861(01)00029-5)
- [18] S.K. Khanna, P. Ranganathan, S.B. Yedla, R.M. Winter, K. Paruchuri, Investigation of Nanomechanical Properties of the Interphase in a Glass Fiber Reinforced Polyester Composite Using Nanoindentation, *J. Eng. Mater. Technol.* 125 (2003) 90–96. <https://doi.org/10.1115/1.1543966>.
- [19] M.R. VanLandingham, J.S. Villarrubia, W.F. Guthrie, G.F. Meyers, Nanoindentation of polymers: an overview, *Macromol. Symp.* 167 (2001) 15–44. [https://doi.org/10.1002/1521-3900\(200103\)167:1<15::AID-MASY15>3.0.CO;2-T](https://doi.org/10.1002/1521-3900(200103)167:1<15::AID-MASY15>3.0.CO;2-T).
- [20] X. Cheng, K.W. Putz, C.D. Wood, L.C. Brinson, Characterization of Local Elastic Modulus in Confined Polymer Films via AFM Indentation, *Macromol. Rapid Commun.* 36 (2015) 391–397. <https://doi.org/10.1002/marc.201400487>.
- [21] A. Hodzic, J.K. Kim, Z.H. Stachurski, Nano-indentation and nano-scratch of polymer/glass interfaces. II: model of interphases in water aged composite materials, *Polymer.* 42 (2001) 5701–5710. [https://doi.org/10.1016/S0032-3861\(01\)00029-5](https://doi.org/10.1016/S0032-3861(01)00029-5).
- [22] Y.-F. Niu, Y. Yan, J.-W. Yao, Hygrothermal aging mechanism of carbon fiber/epoxy resin composites based on quantitative characterization of interface structure, *Polym. Test.* 94 (2021) 107019. <https://doi.org/10.1016/j.polymertesting.2020.107019>.
- [23] Y. Qi, D. Jiang, S. Ju, J. Zhang, X. Cui, Determining the interphase thickness and properties in carbon fiber reinforced fast and conventional curing epoxy matrix composites using peak force atomic force microscopy, *Compos. Sci. Technol.* 184 (2019) 107877. <https://doi.org/10.1016/j.compscitech.2019.107877>.
- [24] Y. Wang, T.H. Hahn, AFM characterization of the interfacial properties of carbon fiber reinforced polymer composites subjected to hygrothermal treatments, *Compos. Sci. Technol.* 67 (2007) 92–101. <https://doi.org/10.1016/j.compscitech.2006.03.030>.
- [25] M. Munz, H. Sturm, E. Schulz, G. Hinrichsen, The scanning force microscope as a tool for the detection of local mechanical properties within the interphase of fiber reinforced polymers, *Compos. Part Appl. Sci. Manuf.* 29 (1998) 1251–1259. [https://doi.org/10.1016/S1359-835X\(98\)00077-3](https://doi.org/10.1016/S1359-835X(98)00077-3).

- [26] A. Afaghi-Khatibi, Y.-W. Mai, Characterisation of fiber/matrix interfacial degradation under cyclic fatigue loading using dynamic mechanical analysis, *Compos. Part Appl. Sci. Manuf.* 33 (2002) 1585–1592. [https://doi.org/10.1016/S1359-835X\(02\)00117-3](https://doi.org/10.1016/S1359-835X(02)00117-3).
- [27] A. Chateauinois, B. Chabert, J.P. Soulier, L. Vincent, Hygrothermal ageing effects on the static fatigue of glass/epoxy composites, *Composites*. 24 (1993) 547–555. [https://doi.org/10.1016/0010-4361\(93\)90268-D](https://doi.org/10.1016/0010-4361(93)90268-D).
- [28] I.B.C.M. Rocha, S. Raijmaekers, R.P.L. Nijssen, F.P. van der Meer, L.J. Sluys, Hygrothermal ageing behaviour of a glass/epoxy composite used in wind turbine blades, *Compos. Struct.* 174 (2017) 110–122. <https://doi.org/10.1016/j.compstruct.2017.04.028>.
- [29] I.R. Chowdhury, N.P. O’Dowd, A.J. Comer, Experimental study of hygrothermal ageing effects on failure modes of non-crimp basalt fiber-reinforced epoxy composite, *Compos. Struct.* 275 (2021) 114415. <https://doi.org/10.1016/j.compstruct.2021.114415>.
- [30] P. Davies, W. Verbouwe, Evaluation of Basalt Fiber Composites for Marine Applications, *Appl. Compos. Mater.* 25 (2018) 299–308. <https://doi.org/10.1007/s10443-017-9619-3>.
- [31] R. Rafiee, M. Maleki, S. Rahnema, Experimental study on the effect of hygrothermal environments combined with the sustained mechanical loads on the strength of composite rings, *Compos. Struct.* 258 (2021) 113397. <https://doi.org/10.1016/j.compstruct.2020.113397>.
- [32] X. Yang, N. Jia, Hygrothermal effect on high-velocity impact resistance of woven composites, *Def. Technol.* 18 (2022) 823–833. <https://doi.org/10.1016/j.dt.2021.03.028>.
- [33] Y. Zhong, M. Cheng, X. Zhang, H. Hu, D. Cao, S. Li, Hygrothermal durability of glass and carbon fiber reinforced composites – A comparative study, *Compos. Struct.* 211 (2019) 134–143. <https://doi.org/10.1016/j.compstruct.2018.12.034>.
- [34] T. Sivasankaraiah, B.R. Lokavarapu, Strength degradation of glass epoxy composites under hygrothermal environment, *Mater. Today Proc.* 38 (2021) 2845–2852. <https://doi.org/10.1016/j.matpr.2020.08.778>.
- [35] P. Siedlaczek, G. Sinn, P. Peter, J. Jandl, G. Hantal, K. Wriessnig, R. Wan-Wendner, H.C. Lichtenegger, Hygrothermal aging of particle-filled epoxy-based composites, *Polym. Degrad. Stab.* 208 (2023) 110248. <https://doi.org/10.1016/j.polymdegradstab.2022.110248>.
- [36] P. Makvandi, M. Ghaemy, M. Mohseni, Synthesis and characterization of photo-curable bis-quaternary ammonium dimethacrylate with antimicrobial activity for dental restoration materials, *Eur. Polym. J.* 74 (2016) 81–90. <https://doi.org/10.1016/j.eurpolymj.2015.11.011>.
- [37] S. Assengone Otogo Be, A. Fahs, L. Belec, S. Belkessam, G. Louarn, J. Chailan, Multiscale investigation of the effect of sizing chemistry on the adhesion and interfacial properties of glass fiber-reinforced epoxy composites, *Polym. Compos.* (2022) pc.27064. <https://doi.org/10.1002/pc.27064>.
- [38] S. Mallarino, J.F. Chailan, J.L. Vernet, Interphase investigation in glass fiber composites by micro-thermal analysis, *Compos. Part Appl. Sci. Manuf.* 36 (2005) 1300–1306. <https://doi.org/10.1016/j.compositesa.2005.01.017>.
- [39] A. Chateauinois, B. Chabert, J.P. Soulier, L. Vincent, Dynamic mechanical analysis of epoxy composites plasticized by water: Artifact and reality, *Polym. Compos.* 16 (1995) 288–296. <https://doi.org/10.1002/pc.750160405>.
- [40] Krauklis, A., Gagani, A., Echtermeyer, A., Long-Term Hydrolytic Degradation of the Sizing-Rich Composite Interphase, *Coatings*. 9 (2019) 263. <https://doi.org/10.3390/coatings9040263>.
- [41] A. Krauklis, A. Gagani, K. Vegere, I. Kalnina, M. Klavins, A. Echtermeyer, Dissolution Kinetics of R-Glass Fibers: Influence of Water Acidity, Temperature, and Stress Corrosion, *Fibers*. 7 (2019) 22. <https://doi.org/10.3390/fib7030022>.

